2015 IEEE International Conference on Robotics and Automation (ICRA), Seattle, Washington, May 26-30, 2015
978-1-4799-6922-7/15/$31.00 ©2015 IEEE

Pulley Friction Compensation for Winch-Integrated Cable Force Measurement and Verification on a Cable-Driven Parallel Robot

Werner Kraus, Michael Kessler and Andreas Pott

***Abstract*— In a cable-driven parallel robot, elastic cables are used to manipulate the end effector within the workspace. Cable force measurement is necessary for several control algorithms like cable force control, contact control, or load identification. The cable force sensor can be placed directly at the connection point on the platform or somewhere along the cable using pulleys. The pulleys between the force sensor and the platform disturb the force measurement accuracy due to friction. This paper deals with modeling and compensation of the friction. The friction behavior in the drive train with focus on the effects of the pulleys is non-trivial, as the cable movement consists of microscopic and macroscopic movements and standstills. Friction models from Coulomb and Dahl are adapted to deal with the pulley friction. The experimental evaluation showed an improvement of 70% with respect to the uncompensated case.**

I. Introduction

Due to their huge workspace, high dynamics and lightweight structure, cable-driven parallel robots, in the following referred to as cable robots, received high interest in the last decades ([1], [2]). The cable robot Mini-IPAnema actuated by eight cables which allows for 6 DoF is shown in Fig. 1.

Cable force measurement is necessary for control of cable forces, measurement of the external forces at the platform for admittance control, or contact control and load identification. It is straightforward to integrate the cable force sensors directly at the attachment point of the cables at the platform. An example can be seen in Fig. 1. As the cable forces are measured directly at the point of interest, one can achieve the highest precision. One the other hand, the cable force sensors and their A/D-converters are part of the moving platform and there has to be an electric connection to the control PC over the field bus. This may lead to an additional source of damage.

To avoid the cable force sensors on the platform (Fig. 2a), the sensors can also be integrated as measurement units using pulleys (Fig. 2b) or integrated in the winch (Fig. 2c). The advantages are that the force sensor is covered and protected and the wiring can be fixed inside the robot frame. It simplifies the assembly of the end effector, as the cable is just connected with a bolt. As the force measurement is now performed within the cable course, the measured cable force does not correspond directly to the force applied to the end effector. The pulleys introduce additional forces like inertia or friction into the cable. In a typical robot design,

This work was supported as a Fraunhofer Master Project.

All the authors are with the Fraunhofer Institute for Manufacturing Engineering and Automation IPA in Stuttgart, Germany
Werner.Kraus at ipa.fhg.de

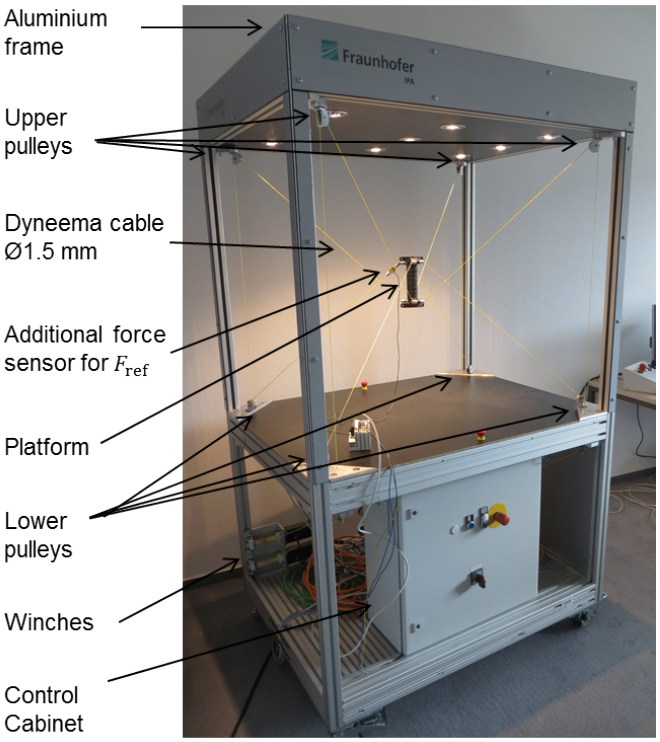

Fig. 1: Cable-driven parallel robot Mini-IPAnema with 8 cables and 6 DoF

multiple pulleys are used to guide the cable, where one to three pulleys lie between the force sensor and the end effector. This leads to disturbed inputs of algorithms based on cable forces. In this paper, we present a friction model for the pulley friction to increase the measurement accuracy.

Friction modeling can be found in several areas of robotics: in humanoid robots, the upper limb is often cable actuated and the load cell is placed in the body. These systems are realized using pulleys or bowden cables. E.g. [3], discrete elements with friction losses are applied for a cable-conduit system used for surgical robots. Viscous and dry friction coefficients are applied in the computed torque control approach for a cable robot [4]. In the cable-driven locomotion interface the Dahl model was applied for the modeling of the reel friction [5].

The challenge for compensating the pulley friction is the high frequent transition between static friction and kinetic friction. The presliding mode needs special consideration [6]. The Coulomb model is not sufficient, as it is stateless and cannot model friction in standstill. Well-known models for

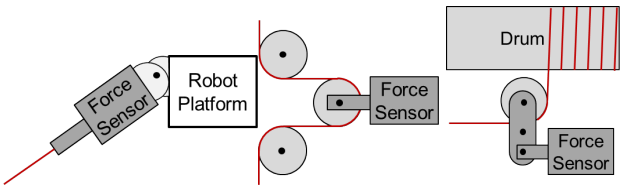

(a) Direct at the platform (b) Using pulleys (c) Winch integrated

Fig. 2: Principles for cable force measurement

dynamic friction are the Dahl and LuGre model [7], [8]. We choose the Dahl model, as it has less parameter and we do not expect stick slip effects.

This paper is structured as follows: The robot model including kinematic and cable force distributions are summarized in section 2. The approach for friction modeling according to Coulomb and Dahl is described in section 3. The parametrization for all cables is presented and the results were discussed. The verification of the model for wrench hysteresis, admittance control and IPAnema 3 winch is described in section 4. Finally, conclusions and an outlook on future works are given in section 5.

II. Robot Model

For completeness, we briefly review the robot model [9]. The geometry of the robot is described by proximal anchor points on the robot base A_i and the distal anchor points on the end effector B_i described by vector $\mathbf{b}_i$. The index i denotes the cable number and m is the absolute number of cables. By applying a vector loop as shown in Fig. 3, the cable vector $\mathbf{l}_i$ follows as

$$\mathbf{l}_i = \mathbf{a}_i(\mathbf{r}, \mathbf{R}) - \mathbf{r} - \mathbf{R}\,\mathbf{b}_i \quad , \tag{1}$$

where $\mathbf{r}$ is the platform position vector and rotation matrix $\mathbf{R}$ describes the platform orientation. As we take the pulleys at winches into account, the vector $\mathbf{a}_i$ to the starting point of the cable depends on the current pose of the robot [10].

The structure equation with the structure matrix $\mathbf{A}^{\mathrm{T}}$ resulting from the force and torque equilibrium at the end effector for the cable force distribution $\mathbf{f}$ is given by

$$\underbrace{\begin{bmatrix} \mathbf{u}_1 & \cdots & \mathbf{u}_m \\ \mathbf{b}_1 \times \mathbf{u}_1 & \cdots & \mathbf{b}_m \times \mathbf{u}_m \end{bmatrix}}_{\mathbf{A}^{\mathrm{T}}(\mathbf{r},\mathbf{R})} \underbrace{\begin{bmatrix} f_1 \\ \vdots \\ f_m \end{bmatrix}}_{\mathbf{f}} = -\underbrace{\begin{bmatrix} \mathbf{f}_p \\ \boldsymbol{\tau}_p \end{bmatrix}}_{\mathbf{w}} \quad , \tag{2}$$

where $\mathbf{u}_i = \frac{\mathbf{l}_i}{\|\mathbf{l}_i\|}$. The wrench $\mathbf{w}$ consists of applied forces $\mathbf{f}_p$ and torques $\boldsymbol{\tau}_p$ and includes also the gravity g.

The wrench $\mathbf{w}$ is derived from

$$\mathbf{w} = -\mathbf{A}^{\mathrm{T}}\mathbf{f}_{\mathrm{is}} \quad , \tag{3}$$

where $\mathbf{f}_{\mathrm{is}}$ corresponds to the measured cable forces.

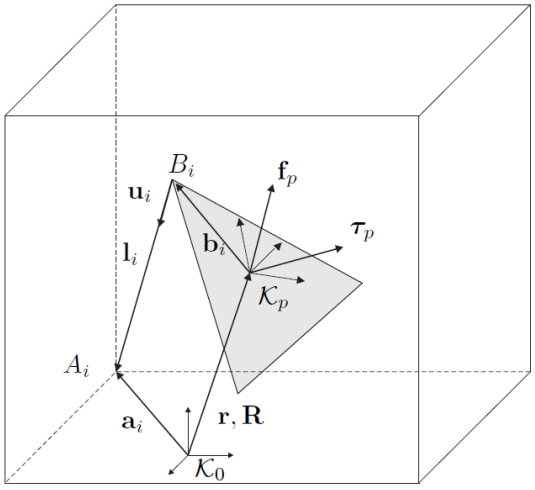

Fig. 3: Description of the robot geometry based on one kinematic loop

III. Pulley Friction Model

A. Coulomb and viscose Friction of a Series of Pulleys

In the following, we derive the basic equations for the determination of the friction forces for a series of pulleys as depicted in Fig. 5. We assume, that the pulleys are always moved by friction due to tension in the cable. Eytelwein's formula with coefficient of friction between the cable and the pulley μ_{p} and wrapping angle α_i of the i^{th} pulley

$$F_j = F_{j-1} e^{\mu_{\mathrm{p}} \alpha} \tag{4}$$

must hold that the friction of the pulley's bearing is dominant, otherwise the cable slides over the pulley what is another type of friction. This includes also the case of cable sagging where the friction drops. In the following, we neglect gravitational sagging and dynamic effects due to wire mass and elasticity.

The force equilibrium for a cable guided around a pulley under the consideration of a friction force $F_{\mathrm{R},j}$ and the cable velocity v can be determined by

$$F_j = F_{j-1} + \mathrm{sgn}(v) F_{\mathrm{R},j} \quad , \tag{5}$$

where F_j and F_{j-1} are the cable forces before and after the pulley, respectively. The friction force of one pulley $F_{\mathrm{R},j}$ is modeled with the Coulomb friction coefficient μ_i and a viscose friction parameter F_{pv} by

$$F_{\mathrm{R},j} = \mu_i F_{\mathrm{N},j} + F_{\mathrm{pv}} |v| \quad , \tag{6}$$

where $F_{\mathrm{N},j}$ is the normal force acting on the bearing. Thus, for the friction estimation, the force acting on the pulley is relevant. In the following, we are using the abbreviations $c\alpha_j = \cos\alpha_j$ and $sv = \mathrm{sgn}(v)$. The normal force $F_{\mathrm{N},j}$ is the sum of incoming and outgoing cable force acting under the actual wrapping angle α_j and is determined by

$$F_{\mathrm{N},j} = \sqrt{F_{j-1}^2 - 2F_{j-1}F_j c\alpha_j + F_j^2} \quad . \tag{7}$$

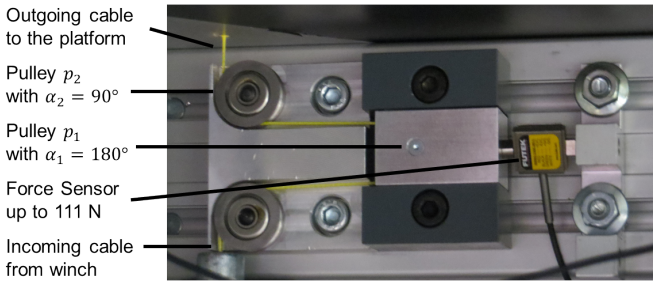

Fig. 4: Pulley unit of mini cable robot for force measurement F_s

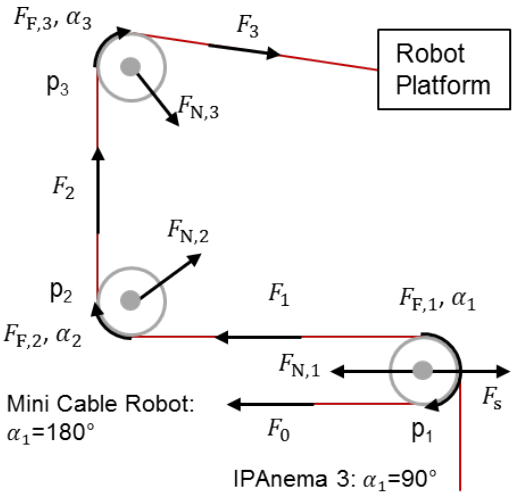

Fig. 5: Course of one cable between the platform and the force sensor guided by three pulleys

The assumption that the normal force vector is the bisection of the wrapping angle allows for the following approximation:

$$F_{\mathrm{N},j} \approx \frac{F_{j-1}+F_j}{2}\sqrt{2(1-c\alpha_j)} \quad . \tag{8}$$

Inserting (8) in (6) and subsequently in (5) results in

$$F_j = F_{j-1} + sv\mu_j \frac{F_{j-1}+F_j}{2}\sqrt{2(1-c\alpha_j)} + F_\mathrm{pv}v \quad , \tag{9}$$

solved for the cable force after pulley F_j yields

$$F_j = \frac{F_{j-1}(2+sv\mu_j\sqrt{2(1-c\alpha_j)})+2F_\mathrm{pv}v}{2-sv\mu_j\sqrt{2(1-c\alpha_j)}} \quad . \tag{10}$$

Because of the force sensor, the first pulley needs special consideration. The force equilibrium for the first pulley along the direction of the force sensor vector F_s is

$$-F_0 c\alpha_1 + F_1 = F_\mathrm{s} \quad . \tag{11}$$

For $\alpha_1 = 90°$ the solution is trivial:

$$F_1(\alpha_1 = 90°) = F_\mathrm{s} \quad , \tag{12}$$

According to (11) for $\alpha_1 = 180°$ $F_0 = F_\mathrm{s} - F_1$ holds. Inserting this into (10) for j=1 yields

$$F_1 = (F_\mathrm{s} - F_1)\frac{1+\mu_1 sv}{1-\mu_1 sv} \quad . \tag{13}$$

Resolved after F_1, the cable force in the first segment returns

$$F_1(\alpha_1 = 180°) = F_\mathrm{s}\frac{1+\mu_1 sv}{2} \quad . \tag{14}$$

To get the cable force acting at the platform, which corresponds to the cable force in the last segment F_{n_p}, one has to evaluate (10) for every pulley starting from F_1. The wrapping angle of the last pulley before the platform α_{n_p} depends on the actual pose of the platform and results from the inverse kinematic. The wrapping angles around the lasting pulleys are defined during installation of the robot and are constant during operation of the robot.

The macroscopic friction F_f of one cable can now be derived with

$$F_\mathrm{f} = F_{n_\mathrm{p}} - F_1 \quad , \tag{15}$$

and is now extended by the Dahl model to deal with both microscopic and macroscopic cable movements.

B. Dahl model

The general form of the Dahl model is a first order differential equation

$$\frac{df}{dx} = \sigma\left[1 - \frac{f}{f_c}\,\mathrm{sgn}(v)\right]^\alpha \quad , \tag{16}$$

where α describes the shape of the hysteresis area. We take $\alpha = 1$ like in other literature ([5], [11], [7]). The basic idea of the Dahl model is to store the friction force acting at a direction change and to apply a smooth transition between the stored and actual calculated friction described by a stiffness value. An implementable solution of the Dahl model is

$$F_\mathrm{d} = F_\mathrm{f}\,\mathrm{sgn}(v_k) + (F_0 + F_\mathrm{f}(\mathrm{sgn}(v_i))e^{-\frac{\sigma}{F_\mathrm{f}}|l-l_0|} \quad , \tag{17}$$

where σ is a design parameter describing the stiffness value of the transition between microscopic and macroscopic movement, l_0 and F_0 representing the actual cable length l and friction force of the Dahl model F_d when the direction of movement changes [11].

C. Identification Experiment

The identification experiment is performed on the completely assembled robot, as shown in Fig. 1. For the identification of the friction between the force signal gained in the measurement unit F_s at the platform, an additional force sensor is attached directly at the platform. In this way, the reference force F_ref is measured, which can be assumed as ideal as there is no friction, except for measurement errors.

The reference trajectory accounts for the identification of the friction during microscopic and macroscopic movements and the transition between them. Movements with small amplitudes and breaks are chosen to stimulate the hysteresis behavior represented by the Dahl model. To account for the viscose friction, the velocity is varied throughout the identification. A distribution in different cable forces and wrapping angles is reached by a trajectory which covers the workspace. In detail, the reference trajectory consists of the following phases.

TABLE I: Final parametrization for all 8 cables based on the reference trajectory and comparison of the model errors

i	μ []	σ [N/mm]	F_{pv} [Ns/m]	$F_{\mathrm{ref}} - F_{\mathrm{s}}$ [N]	$F_{\mathrm{ref}} - F_{\mathrm{s}} - F_{\mathrm{d}}$ [N]	F_{ref} [N]
1	0.016	1.000	1.70	0.46	0.16	8.11
2	0.011	1.003	3.50	0.43	0.21	5.33
3	0.014	0.999	1.55	0.84	0.14	6.54
4	0.017	0.602	1.38	0.49	0.14	8.22
5	0.024	1.000	1.75	0.55	0.18	5.10
6	0.023	0.999	2.08	0.43	0.16	5.83
7	0.024	1.001	1.18	0.44	0.10	3.98
8	0.025	0.998	1.29	0.65	0.24	8.11
mean	0.019	0.950	1.80	0.54	0.17	6.40

- Stop and go movement in the same direction with amplitudes from 0.25 to 10 mm, velocity of 0.083 m/s and a break of 0.5 s. This experiment is conducted in both positive and negative directions.
- Alternating movement with amplitudes from 0.25 to 10 mm, velocity of 0.083 m/s and a break of 0.5 s.
- Alternating movement with an amplitude of 100 mm and rising velocity of 0.167 m/s up to 1.0 m/s.
- Rectangular trajectory with a velocity of 0.167 m/s and 0.5 m/s throughout the workspace.

The commanded cable lengths are derived from inverse kinematics and do not oscillate in standstill of the platform. The movement of the winches is continuous. During the experiments, the cable force control presented in [12] was active to control the cable forces. The cable force control leads to transient set points of the cable lengths. Especially in standstill of the platform, microscopic cable movement is typical due to the interacting cable force controllers. This is important for the sliding mode of the friction model.

D. Final parametrization for all cables

A Levenberg-Marquardt optimization is used for parameter identification for each cable. In the mini cable robot, all pulleys are of equal size and inertia. Thus, we assume the friction coefficient to be the same. The friction depends on the force acting on the bearing. For each cable, the friction model is described with three friction parameters. To deal with calibration difference between the two force sensors, a constant offset ϵ is introduced for the optimization, but neglected in the later implementation. The target function Ψ for the parameter set $p = [\mu\, \sigma\, F_{\mathrm{pv}}\, \epsilon]$ is

$$\min_{p} \sum (\Psi(F_{\mathrm{s}}, v, l, \alpha_{n_{\mathrm{p}}}) + \epsilon - F_{\mathrm{ref}})^2 \quad . \tag{18}$$

For the identification, the reference trajectory is repeated for each cable and the reference sensor is changed from one cable to another. The resulting parameters for the friction model derived by the optimization function can be seen in table I. Also the mean deviation of the real friction error and friction error after compensation are presented.

E. Discussion

The overview over the identified parameters for all 8 cables reveals quite a high variance of the real parameters. The Coulomb friction ranges between 0.011 and 0.025 and the viscose friction between 1.18 and 3.5 Ns/m. The parameter σ is always around 1. The influence of the pulley friction before, $F_{\mathrm{ref}} - F_{\mathrm{s}}$, and after the compensation $F_{\mathrm{ref}} - F_{\mathrm{s}} - F_{\mathrm{d}}$ is also given in table I. In average, the results show a reduction of the error by approximately two thirds. On the other hand this means that one third of the force difference between the two force signals F_{s} and F_{ref} is not included in the model. The mean cable force amounts to 6.40 N, while the friction force created by the pulleys is 0.54 N. Without compensation, the pulley friction disturbs the force measurement by 8.4%.

In the following, we describe some effects by which the model could be extended.

In [13] we discussed the error of the cable force sensor itself. Each force sensor has its one characteristic which may lead to calibration errors. Applying a model between two force sensor signals involves also the measurement errors. In the actual implementation we introduced a constant offset to the target function. A linear model of the force sensor error might be more precise. Otherwise, the calibration differences of the sensors influence the friction parameters.

In [14] we described hysteresis effect of Dyneema cables. We assume that this effect may also influence the cable force measurement over the pulleys. For each cable segment between two pulleys one could apply a separate cable model. In a first approximation, direction-dependent friction parameters could be a practicable approach.

In the previous described approach, the direction of movement of the cable was determined based on the winch direction. This approach is capable to deal with both microscopic and macroscopic cable movement. The state of the $\mathrm{sgn}(v)$ function is crucial for the friction model, as in first approximation holds

$$F_{\mathrm{n_p}} = F_1 + \mathrm{sgn}(v) F_{\mathrm{f}} \quad . \tag{19}$$

A wrong assumption of the direction causes an error of two times the Coulomb friction force f_{f}. When the winch velocity is very small, external force acting at the platform may lead to reversion of the friction at the pulleys. For cable robots this seems to be interesting as the cables are interacting over the platform with each other.

IV. Verification

A. Implementation

The control algorithms are implemented on the cable robot Mini-IPAnema 3 using eight cables and a platform formed like a handle as shown in Fig. 1. The space of the robot's frame is 1.1 m x 0.8 m x 1.0 m. The actuators are 200 W servo drives of type Beckhoff AM3121. Without an additional gear box, the drum with a diameter of 20 mm is connected. The nominal rated cable force neglecting friction amounts to 65 N.

The robot control is realized on a Windows PC with Beckhoff TwinCAT 3.1 CNC at a cycle time of 1 ms. The field bus protocol is EtherCAT. For the force measurement, each cable is equipped with a cable force sensor of type Futek LRM200 with a measurement range of 111 N. The

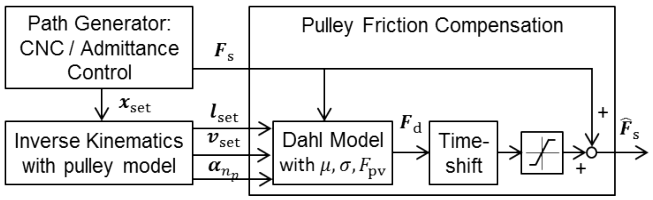

Fig. 6: Structure of the pulley friction compensation implemented in the PLC

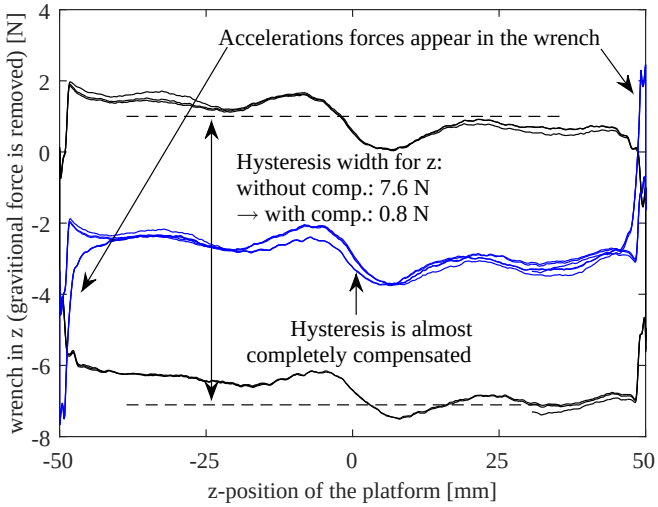

Fig. 7: Reduction of the wrench hysteresis, exemplary in vertical axis

analog output signal of the force sensors is digitized in A/D-converters and sent via the field bus to the control. The cable type is LIROS D-Pro 01505-0150 based on Dyneema SK 75 fibre (Polyethylene) with a diameter of 1.5 mm.

An overview over the implementation of the friction model in the PLC is shown in Fig. 6. The input parameters are the signals of the eight cable force sensor $\mathbf{F}_s$, the set point cable length and velocities of the winches $\mathbf{l}_{set}$, $\mathbf{v}_{set}$ and the pose depending wrapping angle α of the last pulley calculated in the inverse kinematic module. As the velocity set point is used, the model is always ahead of the real friction. Thus, the output of the Dahl model is time-shifted as to correlate the modeled friction with the real effect.

B. Wrench Hysteresis

Beside the control of cable forces, the cable force measurement can also be used to estimate the applied forces on the platform by evaluation of (3). In this way, we estimated the payload on the platform and compensated for the cable elongation in [15]. Using cable force sensors attached directly to the platform, we could improve the relative accuracy under changing load by over 50%. Hysteresis should be very low, otherwise the measured wrench depends on the direction from which the pose is reached. To investigate the influence of pulley friction on the wrench measurement, we programmed the robot to cyclically cross a position in all six DoF.

TABLE II: Improvement of the Wrench hysteresis with and without compensation

Cartesian axis	Hysteresis width [N, Nm] without comp.	with comp.	Lasting Hysteresis [%]
x	7.376	0.979	13.3
y	4.183	0.463	11.1
z	7.619	0.817	10.7
a	0.519	0.165	31.8
b	0.528	0.154	29.2
c	0.111	0.020	18.1

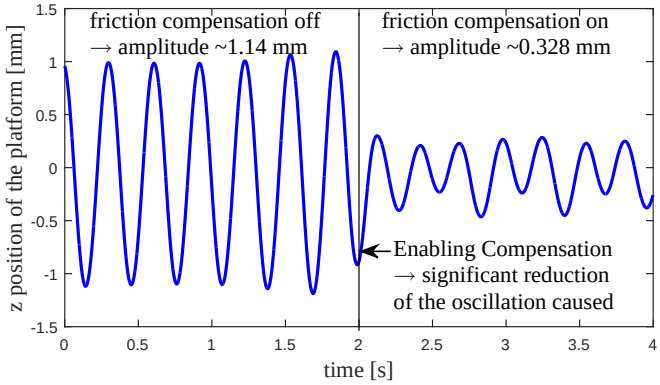

Fig. 8: Reduction of the oscillation of the admittance control in idle mode

The measurement results are summarized in Table II and show the influence of the pulley friction on the measured wrench. The hysteresis ranges in the same dimension as the gravitational force of the unload platform which is 4 N. Especially for translational movements, the friction compensation is able to compensate for a significant part of the Hysteresis. The orientation workspace is quite limited. Therefore, the compensation around the rotation axes a, b and c is comparatively lower.

Exemplary, the hysteresis curve for the investigation of the z-axis of the robot is shown in Fig. 7. Depending on the direction, the wrench changes by 7.6 N. Using the friction compensation, the hysteresis can almost completely compensated to a width of only 0.8 N.

C. Admittance Control

In [16], we presented an admittance control for the Mini IPAnema, which allows for haptic interaction with the cable robot. The user force $\mathbf{w}_{adm}$ is measured and transformed to the set point pose $\mathbf{x}_{set}$ according to a virtual system behavior represented by a spring-mass-damper system

$$\mathbf{I}\ddot{\mathbf{x}}_{set} + \mathbf{D}\dot{\mathbf{x}}_{set} + \mathbf{C}\mathbf{x}_{set} = \mathbf{w}_{adm} \quad , \tag{20}$$

where $\mathbf{I}$, $\mathbf{D}$ and $\mathbf{C}$ are the desired inertia, damping and spring constant, respectively. The user force is measured with the cable force sensors according to (3). Since the cable force sensors were moved from the platform to the indirect measurement over the pulley system, the platform tends to oscillate in idle mode. Actually, in idle mode is no user force and the platform should stand still. The reason for the oscillation lies in the static friction of the pulleys which

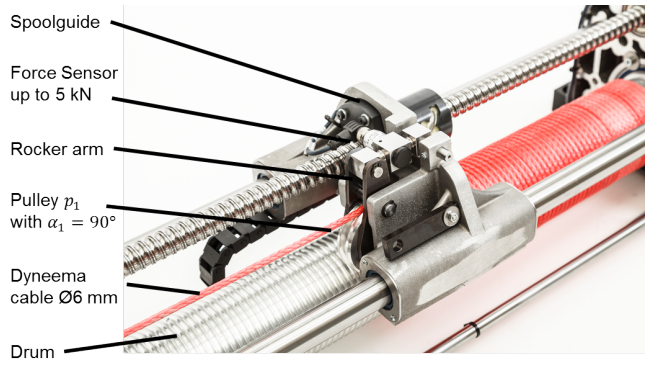

Fig. 9: Winch integrated cable force sensor in IPAnema 3 winch

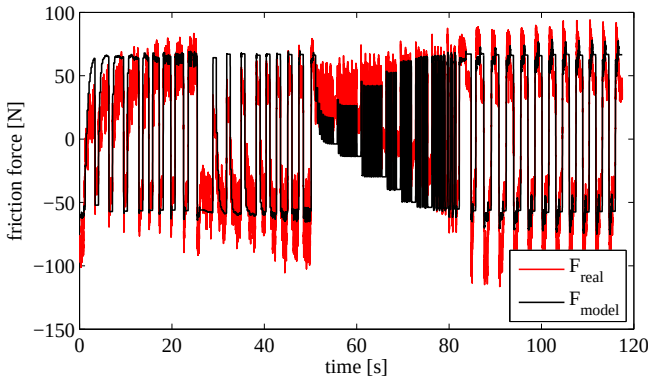

Fig. 10: Friction for the IPAnema 3 winch during handling of 50 kg

is interpreted as user force and turned over in a movement of the platform. Here, the friction compensation also proofs an improvement: The amplitude of the oscillation can be damped by two-thirds from 1.14 mm to 0.328 mm as can be seen in Fig. 8.

D. IPAnema 3 winch

For the IPAnema 3 robot, the force sensor is integrated in the winch as can be seen in Fig. 9. The detailed description of the IPAnema family including the winch can be found in [17]. Here, we present preliminary results regarding friction using only one winch with different loads. For the identification experiment, a load of 210 kg with a velocity of up to 1 m/s was moved using a pulley unit consisting of two pulleys at the ceiling. The reference trajectory consists of microscopic and macroscopic movements. For the IPAnema 3 winch, the identification delivered $\mu = 0.013$, $\sigma = 36.6$ N/mm and F_{pv} =74.5 Ns/m.

For a preliminary verification of the model, a load of 50 kg was applied to the winch. The real friction error and modeled error are shown in Fig. 10. With the friction model, the absolute mean error in the cable force measurement can be reduced from 46.5 to 20.4 N. Roughly calculated, the friction losses amounts 11.6% of the nominal cable force caused by the load.

V. Conclusion

In the paper we analyzed the influence of friction on the control of cable-driven parallel robots. Well-known cable robot demonstrators employ typically one to five pulleys to guide the cable from the actuation to the mobile platform. For a series of pulleys, the basic foundations were derived.

Experimental studies on the IPAnema Mini robot show improvement of round 70 % in the accuracy of the cable force measurement. Initial tests on the large-scale IPAnema 3 system are encouraging. The analysis of the mechanical coupling between the cables and the platform hypothesize a friction effect that is propagated from the platform to the proximal pulleys and which cannot be described with the winch center approach proposed in this paper. Future work may target at analyzing this finding in detail.

References

[1] R. G. Roberts, T. Graham, and T. Lippitt, "On the Inverse Kinematics, Statics, and Fault Tolerance of Cable-Suspended Robots," *Journal of Robotic Systems*, vol. 15, no. 10, pp. 581–597, 1998.

[2] X. Tang, "An Overview of the Development for Cable-Driven Parallel Manipulator," *Advances in Mechanical Engineering*, vol. 2014, no. 10, 2014.

[3] V. Agrawal, W. J. Peine, and B. Yao, "Modeling of Transmission Characteristics Across a Cable-Conduit System," *IEEE Transactions On Robotics*, vol. 26, no. 5, pp. 914–924, 2010.

[4] J. Lamaury, M. Gouttefarde, A. Chemori, and P.-É. Hervé, "Dual-Space Adaptive Control of Redundantly Actuated Cable-Driven Parallel Robots," *IEEE International Conference on Intelligent Robots and Systems*, 2013.

[5] M. J.-D. Otis, T.-L. Nguyen Dang, Laliberte Thiery, D. Quellet, D. Laurendeau, and C. Gosselin, "Cable Tension Control and Analysis of Reel Transparency for 6-DOF haptic foot platform on a cable-driven locomotion interface," *World Academy of Science, Engineering and Technology*, pp. 520–532, 2009.

[6] P. Dupont, V. Hayward, B. Armstrong, and F. Altpeter, "Single state elastoplastic friction models," *IEEE Transactions on Automatic Control*, vol. 47, no. 5, pp. 787–792, 2002.

[7] C. Canudas de Wit, H. Olsson, K. J. Aström, and P. Lischinsky, "A new model for control of systems with friction," *IEEE Transactions on Automatic Control*, vol. 40, no. 3, pp. 419–425, 1995.

[8] P. R. Dahl, "A solid friction model," *The Aerospace Corporation*, 1968.

[9] R. Verhoeven, "Analysis of the Workspace of Tendon-based Stewart Platforms," Ph.D. dissertation, University of Duisburg-Essen, Duisburg, 2004.

[10] A. Pott, "Influence of Pulley Kinematics on Cable-Driven Parallel Robots," in *Latest Advances in Robot Kinematics*, 2012, pp. 197–204.

[11] M. Mahvash and A. M. Okamura, "Friction compensation for a force-feedback telerobotic system," *IEEE International Conference on Robotics and Automation*, pp. 3268–3273, 2006.

[12] W. Kraus, V. Schmidt, P. Rajendra, and A. Pott, "System Identification and Cable Force Control for a Cable-Driven Parallel Robot with Industrial Servo Drives," *IEEE International Conference on Robotics and Automation*, 2014.

[13] ——, "Load identification and compensation for a Cable-Driven parallel robot," *IEEE International Conference on Robotics and Automation*, pp. 2485–2490, 2013.

[14] P. Miermeister, W. Kraus, T. Lan, and A. Pott, "An Elastic Cable Model for Cable-Driven Parallel Robots Including Hysteresis Effects," *Cable-Driven Parallel Robots*, 2014.

[15] W. Kraus and A. Pott, "Load identification and compensation for a Cable-Driven parallel robot," *IEEE International Conference on Robotics and Automation*, pp. 2485–2490, 2013.

[16] W. Kraus, A. Mangold, W. Y. Ho, and A. Pott, "Haptic Interaction with a Cable-Driven Parallel Robot Using Admittance Control," in *Cable-Driven Parallel Robots*, 2015, pp. 201–212.

[17] A. Pott, H. Mütherich, W. Kraus, V. Schmidt, P. Miermeister, and A. Verl, "IPAnema: A family of Cable-Driven Parallel Robots for Industrial Applications," *Cable-Driven Parallel Robots*, 2012.